Radiation Pattern Synthesis of Folded Geodesic Lens Antennas

Germán León[1], Susana Loredo[1], Enrique G. Plaza[2], Set Pérez-González[3]
[1] Dept. of Electrical Engineering, Universidad de Oviedo, Gijón, Spain, gleon@uniovi.es, loredosusana@uniovi.es
[2] Area of Applied Physics, Dept. Of Physics, Universidad de Oviedo, Gijón, Spain, gonzalezenrique@uniovi.es
[3] Area of Applied Mathematics, Dept. Of Mathematics, Universidad de Oviedo, Gijón, Spain, perezset@uniovi.es

***Abstract*—The fifth and sixth generation of mobile communication systems will allow the development of several new services. New millimetre-wave multibeam antennas are needed to provide wide and stable beams. Rotationally symmetric geodesic lens antennas (GLA) can fulfil these requirements. In this work, a two-step method to design folded GLAs is presented. In the first step, a folded focusing lens is searched such that its radiation pattern minimizes a cost function. In the second step, a genetic algorithm is run to diminish the value of the cost function. As an example, this method has been used to design a GLA with 24º of beamwidth and side lobe level below -15 dB. A multibeam antenna has been simulated based on this lens. The antenna is fed by nine ports, which ensures high overlapping between independent beams. This antenna can provide a coverage of 110º.**

***Index Terms*— 5G and beyond, multibeam antennas for base stations, geodesic lens, radiation pattern synthesis.**

INTRODUCTION

The fifth generation (5G) of mobile communication systems is now commercially available. In parallel to this industrial maturity, the expansion of systems beyond 5G, known as the sixth generation (6G) of wireless systems, are growing (see [1]-[3] and the references within). Both systems propose the improvement of several communication services (ultra-dense networks, ultra-reliable, massive machine communications, massive MIMO, …) based, among others, in the use of new and higher frequency bands.

Millimetre-wave (mmWave) technologies play an important role in the expansion of the present and future networks. These systems need new base stations (BSs) that require broadband mmWave antennas with dual-polarization and wide and stable beams. Some of these requirements can be fulfilled by electronically steerable beam antennas [4-6] or by multibeam antennas ([7] and its references within).

Lens based antennas are excellent candidates as mmWave multibeam antennas [8-12] and they may cover a wide field of view. These antennas may generate multiple simultaneous beams from a same aperture, subdividing the service area and enabling spectrum re-use in adjacent cells. In this context, geodesic lens-based antennas (GLA) are a new class of fully metallic parallel plate waveguide antennas [13-15], which have demonstrated good scanning properties up to 60º, in addition to simplicity and low losses. Different radiation patterns can be obtained by varying the lens profile. For example, a GLA with a beamwidth of 20º for 5G applications was developed in [15]. Furthermore, these lenses can concentrate the rays in one or two points in the near field of the antenna.

Usually, these lenses feature rotational symmetry, but other topologies are under study. In this contribution, only rotationally symmetrical lenses are considered, in order to generate multiple stable beams. The authors present a radiation pattern synthesis algorithm for folded GLA. In this algorithm a geodesic lens (GL) profile is described in terms of spline curves, generalizing the method used in [12]. The radiation pattern of a generic GLA is determined using the hybrid model developed in [14]. The lens profile can be modulated in order to find a specific radiation pattern. The proposed algorithm allows us to design the GLA taking into account the desired beamwidth and side lobe level (SLL).

GEODESIC LENS ANTENNA DESIGN

A. Brief description of the GLA Hybrid Model

GLAs can be constructed using parallel plate waveguide technology, where the fields are confined between two metallic plates. GLs are typically defined in terms of the radial coordinate ρ, the angular coordinate ϕ, and the length on the surface measured along the meridian from the axis $s(\rho)$:

$$ds^2(\rho) = d\rho^2 + dz^2(\rho), \tag{1}$$

where $z(\rho)$ is the height of lens, that defines the lens profile. The radiation pattern of a GLA can be modelled with a ray-tracing model [15]. The rays emerge from a source point P_I ($\rho = R_L$, $\phi = \pi$, $z = 0$) with an angle α_i, and travel through the lens maintaining a constant angular momentum L_i:

$$L_i = R_L \sin(\alpha_i) = \rho \sin(\alpha), \tag{2}$$

Each ray travels through the lens diminishing its radial coordinate ρ and varying the angle between the meridian and the ray, α, in such a way that the angular momentum remains constant. When α achieves the value of 90º, the ray reaches the turning point, so the value of ρ increases again until the ray arrives at the end of the lens aperture, with a final radial position ϕ_i and having travelled a distance σ_i:

$$\phi_i = 2 \cdot \int_{L_i}^{R_L} \frac{L_i s'(\rho) d\rho}{\rho \sqrt{\rho^2 - L_i^2}} - \pi \quad (3)$$

$$\sigma_i = 2 \cdot \int_{L_i}^{R_L} \sqrt{s'(\rho)^2 \left(1 + \frac{L_i^2}{\rho^2 - L_i^2}\right)} d\rho \quad (4)$$

where $s'(\rho) = ds/d\rho$ is the derivate of the function $s(\rho)$. This aperture can be modelled as an array of Huygen's secondary sources, and the radiation pattern can be computed by summing up the contributions of all the sources [15]. The algorithm requires less than 20s on a conventional desktop computer to calculate the radiation pattern of a GLA. Fig. 1 depicts the tops view of the physical behaviour of the ray inside the GL.

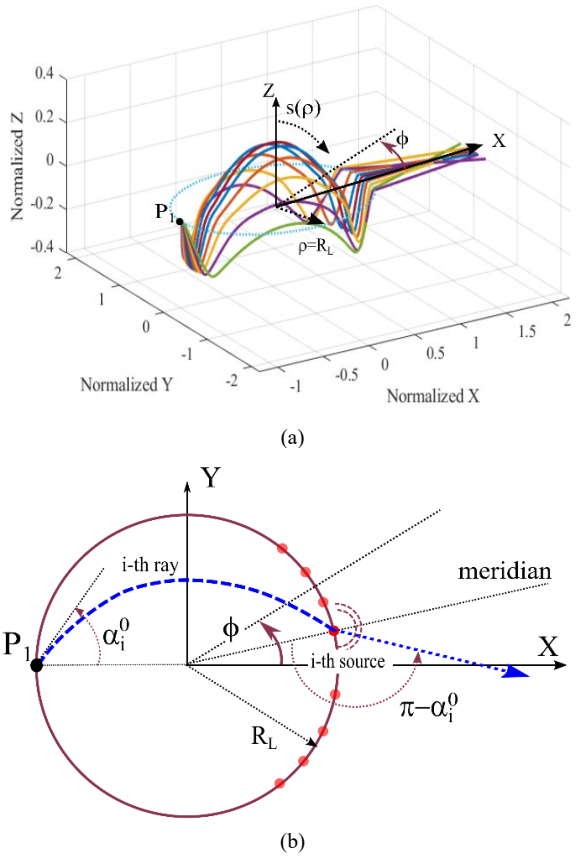

Fig. 1. a) Ray tracing of a folded GLA. b) Scheme of ray tracing model inside and outside the lens.

B. *Spline definition of the Geodesic Lens*

GLs can modulate the delay of the rays, changing their physical paths, through the absolute value of the variation of the lens profile. This variation can be continuous, only limited by the precision in the manufacturing process. Eq.(1) shows that variations in the profile can be either positive or negative, but the change in the path depends only on the absolute value. This allows for the design of a folded lens, which makes the final antenna more compact.

In [14], second order spline curves are applied to define the GL. In that work, the points that define the splines are not equidistant to reduce the number of splines, taking advantage of prior knowledge of the lens profile. In this contribution, the authors present a different approach: we use a number N_s of equidistant cubic splines, in order to be able to generate a great variety of lens profiles.

C. *Guided Genetic Algorithm*

Once the lens radius R_L and the number N_s of splines are fixed, a general-purpose search algorithm could be used to find a radiation pattern that fulfils certain requirements. However, that algorithm might provide solutions with a highly variable profile, which could produce internal reflections inside the lens. The aforementioned hybrid model does not take into account such reflections. So, in this work, we present a two-step approach. We take in advance that Near-Field (NF) focusing GLA can provide a great variety of Far-Field (FF) radiation patterns by simply varying two parameters: the focusing point ρ_2 and the change in the polar angle M [15-16].

Then, in the first step, we iteratively vary the values of ρ_2 and M, fold the lens with N_s splines and run the model described in the previous subsection, monitoring the FF to find the pattern for which the defined cost function reaches its minimum value. It has to be highlighted that folded GLA with the same values of ρ_2 and M, but different number of splines can provide different radiation patterns. For the different cases analysed so far, and particularly for the example presented in this work, $N_s = 8$ has satisfactorily fitted the FF pattern into the imposed requirements. For $N_s < 6$ the lens profile departs substantially form the exact one, as can be observed in Fig. 2, while for $N_s > 12$ the curvature radius at the point where the lens is folded is very small, giving rise to a very abrupt variation, which can generate unwanted reflections. This first step ensures then to find a compact solution with a low value of internal reflections.

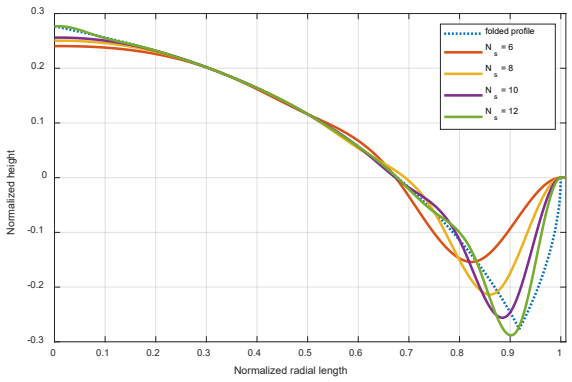

Fig. 2. Comparison between an exact folded (dotted line) and some profiles based on spline approximation

The second step consists of a fine tuning to improve the solution found in the first step. For this purpose, the lens profile obtained in first step is used as a seed to generate a set of possible solutions. These are obtained by allowing random

variations, in a limited interval, of the amplitude values at the points defining the splines, thus generating a sort of tube of curves, as shown in Fig. 3. From this initial set, a genetic algorithm is run to improve the initial solution, allowing only profiles inside this tube, which can be narrowed in successive iterations to further confine the search. This second step guarantees a solution with minimum cost value within this solution set.

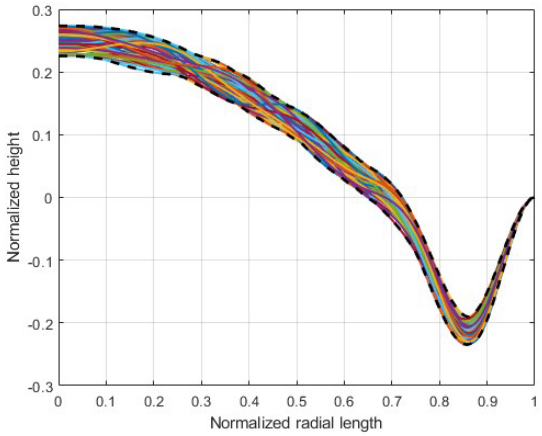

Fig.3. Possible lens profiles, forming a tube.

RESULTS

A. *Flat-top geodesic lens*

The described algorithm has been applied to the design of a folded geodesic lens at the frequency of 38 GHz, exhibiting a flat-top beam pattern with a beamwidth of 24° and SLL of -15 dB. These requirements have been translated into the upper and lower masks, $M^{up}(\phi)$ and $M^{low}(\phi)$ respectively, to be used by the algorithm to achieve the desired radiation pattern. The lens radius was set to 50 mm.

The cost function is given by

$$C = \sum_{m=1}^{M} |E_k - M_k|, \tag{5}$$

where E_k and M_k are the computed and mask fields at the sampled points. If $E_k > M_k^{up}$, then $M_k = M_k^{up}$, but if $E_k < M_k^{low}$, then $M_k = M_k^{low}$. When $M_k^{low} \leq E_k \leq M_k^{up}$, the cost value is zero for that sampled point.

After the first step, the best solution was found for $\rho_2 = 2.5$ and $M = 1.03$, with a cost value of 0.095 Then, in the second step, a set of sixty curves was initially generated around the lens profile given by this solution, and the genetic algorithm was run to improve the result. In this case, three rounds of the algorithm with five iterations each were implemented. In addition, each round further narrowed the search space, so that the range of variation of the generated curves became smaller and smaller.

The algorithm was run ten times to study the behaviour of the cost function. Its value was found to be less than 0.02 in all cases, being between 0 and 0.01 in seven of the runs. Fig. 4 shows one of these results (blue colour), together with the used masks. Its cost value is 0.00075.

The number of turns and iterations, as well as the search space, may depend on the goodness of the solution from the first step. When its cost value is already small, the search for the final solution is done in a smaller space and is faster, requiring fewer iterations.

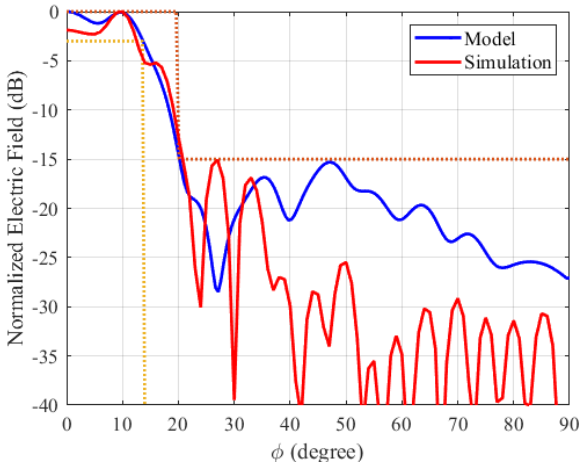

Fig.4. Radiation pattern comparison for the hybrid model and full-wave simulations.

B. *Final Multibeam antenna*

The synthesized lens has been used to design a multibeam antenna for MIMO applications (Fig. 5). The lens is fed by nine independent ports, with a separation of 11º, so the suggested antenna presents a high overlapping between adjacent beams. The hybrid model result has been contrasted with ANSYS HFSS simulation. Fig. 4 includes the normalized radiation pattern of the lens antenna when it is fed by the centre port (port 5). The simulated result has good match with the proposed mask.

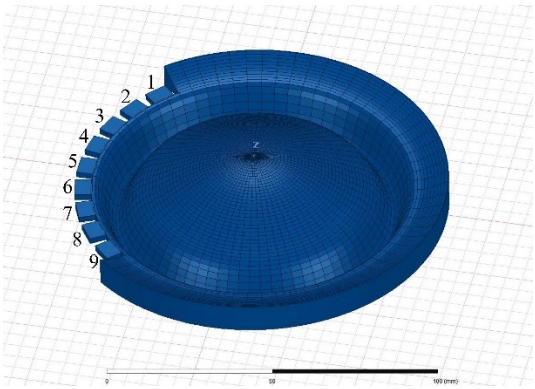

Fig.5. Final design of a GLA with a beamwidth of 24º.

The realized gain of the nine ports is shown in Fig. 6. The beam shape of all ports remains stable, due to the rotational symmetry. This multibeam antenna provides a total coverage of ± 55º. Moreover, within a range of ± 40º, any direction can be covered by two different beams. The coverage of the

multibeam antenna could be increased, adding new ports, but the beams would be slightly deformed.

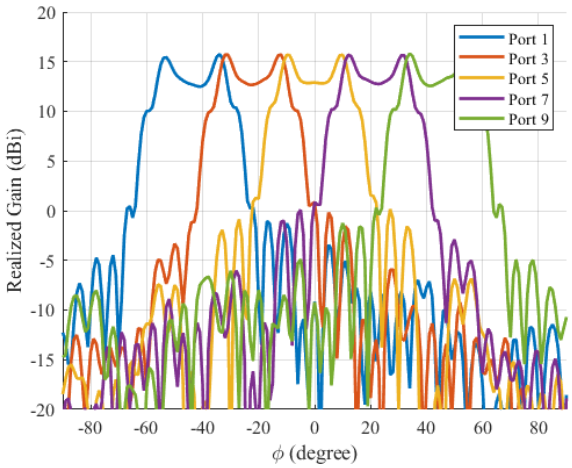

(a)

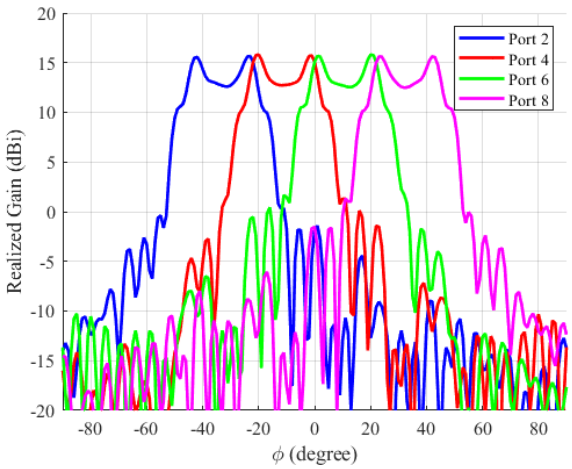

(b)

Fig. 6 Realized gain of the GLA with 9 independent ports.

CONCLUSIONS

In this work, we proposed a method to design compact GLA with a desired radiation pattern. The synthesis algorithm consists of two steps. First, a NF lens is folded, and its profile is modified, varying two parameters, in order to find the most suitable radiation pattern. Once a profile is selected, a fine tuning based on a genetic algorithm is carried out. This algorithm has been applied to find a GLA with a beamwidth of 24° and SLL of -15 dB. This method only takes five minutes to find a GLA that fulfils the requirements.

Furthermore, a GLA with nine independent beams has been simulated. Very good matching is found between the model and the full-wave simulations. A total coverage of ± 55º can be found and a wide area of overlapping beams.

ACKNOWLEDGMENT

This research was supported in part by the Ministerio de Ciencia e Innovación under Project PID2020-114172RB-C21 (ENHANCE-5G), by the Gobierno del Principado de Asturias and Fondo Europeo de Desarrollo Regional (FEDER) under Project grant AYUD/2021/51706, and by Vicerrectorado de Investigación of Universidad de Oviedo under Plan de Apoyo y Promoción de la Investigación under Project Papi21-GR-2010-0015

REFERENCES

[1] W. Hong et al., "The Role of Millimeter-Wave Technologies in 5G/6G Wireless Communications", IEEE Journal of Microwaves, vol. 1, no. 1, pp. 101-122, Jan. 2021, doi: 10.1109/JMW.2020.3035541.

[2] H. Tataria, M. Shafi, A. F. Molisch, M. Dohler, H. Sjöland and F. Tufvesson, "6G Wireless Systems: Vision, Requirements, Challenges, Insights, and Opportunities", Proceedings of the IEEE, vol. 109, no. 7, pp. 1166-1199, July 2021, doi: 10.1109/JPROC.2021.3061701.

[3] H. Tataria, M. Shafi, M. Dohler and S. Sun, "Six Critical Challenges for 6G Wireless Systems: A Summary and Some Solutions", IEEE Vehicular Technology Magazine, vol. 17, no. 1, pp. 16-26, March 2022, doi: 10.1109/MVT.2021.3136506.

[4] J. Ala-Laurinaho et al., "2-D Beam-Steerable Integrated Lens Antenna System for 5G E-Band Access and Backhaul", IEEE Trans. Microw. Theory Tech., vol. 64, no. 7, pp. 2244-2255, July 2016, doi: 10.1109/TMTT.2016.2574317.

[5] B. Yang, Z. Yu, Y. Dong, J. Zhou and W. Hong, "Compact Tapered Slot Antenna Array for 5G Millimeter-Wave Massive MIMO Systems", IEEE Trans. Antennas Propag., vol. 65, no. 12, pp. 6721-6727, Dec. 2017, doi: 10.1109/TAP.2017.2700891.

[6] K. -M. Mak, K. -K. So, H. -W. Lai and K. -M. Luk, "A Magnetoelectric Dipole Leaky-Wave Antenna for Millimeter-Wave Application", IEEE Trans. Antennas Propag., vol. 65, no. 12, pp. 6395-6402, Dec. 2017, doi: 10.1109/TAP.2017.2722868.

[7] W. Hong et al., "Multibeam Antenna Technologies for 5G Wireless Communications", IEEE Trans. Antennas Propag., vol. 65, no. 12, pp. 6231-6249, Dec. 2017, doi: 10.1109/TAP.2017.2712819.

[8] M. A. B. Abbasi, V. F. Fusco, H. Tataria and M. Matthaiou, "Constant-ϵ_r Lens Beamformer for Low-Complexity Millimeter-Wave Hybrid MIMO", IEEE Trans. Microw. Theory Tech., vol. 67, no. 7, pp. 2894-2903, July 2019, doi: 10.1109/TMTT.2019.2903790.

[9] O. Quevedo-Teruel et al., "Geodesic Lens Antennas for 5G and Beyond", IEEE Commun. Mag., vol. 60, no. 1, pp. 40-45, January 2022, doi: 10.1109/MCOM.001.2100545.

[10] Y. Li, L. Ge, M. Chen, Z. Zhang, Z. Li and J. Wang, "Multibeam 3-D-Printed Luneburg Lens Fed by Magnetoelectric Dipole Antennas for Millimeter-Wave MIMO Applications", IEEE Trans. Antennas Propag., vol. 67, no. 5, pp. 2923-2933, May 2019, doi: 10.1109/TAP.2019.2899013.

[11] O. Quevedo-Teruel, J. Miao, M. Mattsson, A. Algaba-Brazalez, M. Johansson and L. Manholm, "Glide-Symmetric Fully Metallic Luneburg Lens for 5G Communications at Ka-Band", IEEE Antennas Wirel. Propag. Lett., vol. 17, no. 9, pp. 1588-1592, Sept. 2018, doi: 10.1109/LAWP.2018.2856371.

[12] H. -T. Chou, Y. -S. Chang, H. -J. Huang, Z. -D. Yan, T. Lertwiriyaprapa and D. Torrungrueng, "Optimization of Three-Dimensional Multi-Shell Dielectric Lens Antennas to Radiate Multiple Shaped Beams for Cellular Radio Coverage", IEEE Access, vol. 7, pp. 182974-182982, 2019, doi: 10.1109/ACCESS.2019.2959277.

[13] Q. Liao, N. J. G. Fonseca and O. Quevedo-Teruel, "Compact Multibeam Fully Metallic Geodesic Luneburg Lens Antenna Based on Non-Euclidean Transformation Optics", IEEE Trans. Antennas Propag., vol. 66, no. 12, pp. 7383-7388, Dec. 2018, doi: 10.1109/TAP.2018.2872766.

[14] N. J. G. Fonseca, Q. Liao and O. Quevedo-Teruel, "Equivalent Planar Lens Ray-Tracing Model to Design Modulated Geodesic Lenses Using Non-Euclidean Transformation Optics", IEEE Trans. on Antennas Propag., vol. 68, no. 5, pp. 3410-3422, May 2020, doi: 10.1109/TAP.2020.2963948.

[15] O. Orgeira, G. León, N. J. G. Fonseca, P. Mongelos and O. Quevedo-Teruel, "Near-Field Focusing Multibeam Geodesic Lens Antenna for Stable Aggregate Gain in Far-Field", IEEE Trans. Antennas Propag.,

vol. 70, no. 5, pp. 3320-3328, May 2022, doi: 10.1109/TAP.2021.3139093.

[16] G. León, O. Orgeira, N. J. G. Fonseca and O. Quevedo-Teruel, "Stacked Geodesic Lenses for Radar Applications in the W-Band", 2022 16th European Conference on Antennas and Propagation (EuCAP), 2022, pp. 1-5, doi: 10.23919/EuCAP53622.2022.9769009.